Articles

Kinetics of Halide Release of Haloalkane Dehalogenase: Evidence for a Slow Conformational Change[†]

Joost P. Schanstra and Dick B. Janssen*

Department of Biochemistry, Groningen Biomolecular Sciences and Biotechnology Institute, University of Groningen, Nijenborgh 4, 9747 AG Groningen, The Netherlands

Received December 11, 1995; Revised Manuscript Received March 11, 1996[⊗]

ABSTRACT: Haloalkane dehalogenase converts haloalkanes to their corresponding alcohols and halides. The reaction mechanism involves the formation of a covalent alkyl−enzyme complex which is hydrolyzed by water. The active site is a hydrophobic cavity buried between the main domain and the cap domain of the enzyme. The enzyme has a broad substrate specificity, but the k_{cat} values of the enzyme for the best substrates 1,2-dichloroethane and 1,2-dibromoethane are rather low (3 and 3.5 s^{-1}, respectively). Stopped-flow fluorescence experiments with substrate under single-turnover conditions indicated that halide release could limit the overall k_{cat}. Furthermore, at 5 mM 1,2-dibromoethane the observed rate of substrate binding to free enzyme was faster than 700 s^{-1} (within the dead time of the stopped-flow instrument) whereas displacement of halide by 5 mM 1,2-dibromoethane occurred at a rate of only 8 s^{-1}. The binding of bromide and chloride to free enzyme was also studied using stopped-flow fluorescence, and the dependence of k_{obs} on the halide concentration suggested that there were two parallel routes for halide binding. One route, in which a slow enzyme isomerization is followed by rapid halide binding, was predominant at low halide concentrations. The other route involves rapid binding into an initial collision complex followed by a slow enzyme isomerization step and prevailed at higher halide concentrations. The overall rate of halide release was low and limited by a slow enzyme isomerization preceding actual release (9 and 14.5 s^{-1} for bromide and chloride, respectively). We propose that this slow isomerization is a conformational change in the cap domain that is necessary to allow water to enter and solvate the halide ion. A solvent kinetic isotope effect of ^2H_2O was found both on k_{cat} and on the rate of halide release. ^2H_2O mainly affected the rate of the conformational change, which is in agreement with this step being rate-limiting and the overall stabilizing effect of ^2H_2O on the conformation of proteins.

Haloalkane dehalogenase from *Xanthobacter autotrophicus* GJ10 hydrolyzes haloalkanes to alcohols and halides. The active site is buried and located between a globular main domain and a largely α-helical cap domain (Verschueren et al., 1993a). The main domain has a typical α/β-hydrolase fold, which is also found in several other hydrolytic enzymes (Ollis et al., 1992). These enzymes have a similar topological arrangement of the active site residues, although they often have very little sequence similarity. The active site cavity of haloalkane dehalogenase is mainly lined with hydrophobic residues. The only hydrophilic amino acids are the catalytic residues Asp124, His289, and Asp260.

The reaction mechanism was deduced from X-ray crystallographic studies on enzyme soaked in substrate (Verschueren et al., 1993b) and site-directed mutagenesis studies (Pries et al., 1994a, 1995a,b). Asp124 is the nucleophile causing the release of the halide ion and formation of a covalent alkyl−enzyme intermediate. This step is preceded by noncovalent binding of the substrate into the Michaelis complex (Verschueren et al., 1993b). The leaving group ($Cl_α$) of the substrate is bound by two tryptophan residues (Trp125 and Trp175). X-ray crystallographic experiments and fluorescence studies showed that the liberated halide ion can also bind at this position (Verschueren et al., 1993c). Mutation of these residues leads to a significant loss of catalytic activity and a reduced affinity for halides (Kennes et al., 1995). After nucleophilic displacement of the halogen the next step in the reaction mechanism is hydrolysis of the alkyl−enzyme intermediate by activated water. With the assistance of Asp260, His289 acts as a general base catalyst to abstract a proton from a water molecule (Verschueren et al., 1993b; Pries et al., 1995a). The high nucleophilicity of this water molecule was shown by rapid reappearance of active Asp124 enzyme by hydrolytic deamidation of the inactive Asp124Asn mutant of the dehalogenase (Pries et al., 1995b). Only the chloride ion positioned between the two tryptophan residues was found back in the X-ray structure after hydrolysis of the alkyl−enzyme intermediate (Verschueren et al., 1993b). The alcohol produced by hydrolysis of the intermediate was never observed, indicating that as soon as this uncharged polar product is formed it diffuses out of the hydrophobic active site cavity.

The fluorescence of the two binding site tryptophans is quenched upon binding of halides (Verschueren et al., 1993c). Titration of the enzyme with halide results in a

[†] This work was supported by a grant from the Biotechnology Programme of the Dutch Ministry of Economic Affairs.

* Address correspondence to this author. Tel: 31-50-3634208. FAX: 31-50-3634165. E-mail: d.b.janssen@chem.rug.nl.

[⊗] Abstract published in *Advance ACS Abstracts,* April 15, 1996.

S0006-2960(95)02904-7 CCC: $12.00

typical ligand binding curve from which the dissociation constant (K_d) of this ligand can be calculated. The fraction of accessible tryptophans (f_a) for the ligand can also be determined in this way. For the wild type dehalogenase, this is one-third, in agreement with the total number of six tryptophans in the enzyme (Verschueren et al., 1993c; Kennes et al., 1995).

The observation that halide was bound between the two substrate binding site tryptophans in the X-ray structure after completion of the chemical part of the reaction may indicate that release of the charged halide from the active site could be one of the slow steps in the reaction sequence. Steady-state dissociation constants of bromide and chloride differ by an order of magnitude (Kennes et al., 1995), whereas the conversion rates for the corresponding substrates 1,2-dibromoethane and 1,2-dichloroethane are nearly the same, however. This suggests that there is no direct correlation between the affinity of the enzyme for halides and the k_{cat}.

To obtain an understanding of the kinetics of halide release and its effect on the k_{cat}, we studied the kinetics of this process using stopped-flow fluorescence. The results indicate that the rate of halide dissociation is limited by a slow conformational change and that the kinetics of this process limits the steady-state turnover rate.

MATERIALS AND METHODS

Materials. Halogenated compounds were obtained from Janssen Chimica, Beerse (Belgium), or from Merck, Darmstadt (FRG). ^2H_2O (99.8% v/v) was purchased from Merck or Isotec, Inc., Miamisburg, OH (U.S.A.).

Dehalogenase was produced using plasmid pGELAF+ in *Escherichia coli* strain BL21(DE3) (Studier et al., 1990). pGELAF+ is an expression vector based on pET-3d (Studier et al., 1990) with the dehalogenase gene (*dhlA*) under control of the T7-promoter and an additional f(1)+ origin for the production of single-stranded DNA (Schanstra et al., 1993).

Protein Expression and Purification. The enzyme was expressed and purified as described earlier (Schanstra et al., 1993). The buffers used during purification were TEMAG [10 mM Tris-sulfate, pH 7.5, 1 mM EDTA, 1 mM 2-mercaptoethanol, 3 mM sodium azide, and 10% (v/v) glycerol] and PEMAG [10 mM sodium phosphate pH 6.0, 1 mM EDTA, 1 mM 2-mercaptoethanol, 3 mM sodium azide, and 10% (v/v) glycerol] for DEAE cellulose chromatography and hydroxylapatite chromatography, respectively. The enzyme was concentrated with an Amicon ultrafiltration cell using a PM10 filter and stored in TEMAG buffer at 4 °C.

Dehalogenase Assays and Protein Analysis. Dehalogenase assays were performed at 30 °C using colorimetric determination of halide release from 5 mM substrate dissolved in 50 mM Tris-sulfate, pH 8.2, as described by Keuning et al. (1985). Solvent kinetic isotope effects were determined with substrate dissolved in ^2H_2O. Assays were performed as described above using increasing concentrations of ^2H_2O.

Protein concentrations of crude extracts were determined with Coomassie Brilliant Blue with bovine serum albumin as a standard. The concentration of pure enzyme was determined spectrophotometrically using $\epsilon_{280} = 4.87 \times 10^4$ M^{-1} cm^{-1} calculated with the program DNASTAR (DNASTAR Inc., Madison, WI). The isolated enzyme was analyzed with SDS−PAGE, which showed that the purity of the preparations was greater than 98%.

Steady-State Halide Binding. Steady-state halide binding was measured by determination of fluorescence quenching on a SLM Aminco SPF500-C spectrofluorimeter at 30 °C. Before the experiment, the enzyme was dialyzed at least 3 h against a 1000-fold larger volume of TEMA (50 mM Tris-sulfate, pH 8.2, 1 mM EDTA, 1 mM 2-mercaptoethanol, and 3 mM sodium azide) to remove the glycerol. Immediately prior to the experiment the enzyme was diluted to 1 mM. Halides were added from freshly prepared stock solutions of NaCl or KBr in the same buffer as the enzyme. The decrease in fluorescence was corrected for dilution, which did not exceed 10%. The excitation wavelength was at 290 nm, and spectra were recorded in the range 300−500 nm.

Stopped-Flow Fluorescence Quenching Experiments. Stopped-flow fluorescence was used to study the kinetics of halide and substrate binding. All experiments were performed on an Applied Photophysics model !SX17MV stopped-flow spectrofluorimeter fitted with a Xe arc lamp with excitation at 290 nm. Fluorescence emission from Trp residues was observed through a 320 nm cutoff filter supplied with the stopped-flow instrument. All reactions were performed at 30 °C, and the reported concentrations are those in the reaction chamber. Each trace shown is the average of four to seven individual experiments (depending on the signal). Prior to each experiment the enzyme was dialyzed for at least 3 h against 1000 volumes of TEMA to remove the glycerol.

Data Analysis. Apparent steady-state dissociation constants were determined by nonlinear regression fitting (Sigmaplot V2.0, Jandel Scientific) of the equation $(F_0 - F)/F_0 = f_a[X]/([X] + K_d)$, where F is the observed fluorescence at halide concentration [X], K_d is the apparent dissociation constant, and f_a is the fraction of the total fluorescence that is quenched at $[X] \gg K_d$.

Stopped-flow kinetic traces of halide binding were analyzed by a nonlinear regression routine implemented in the stopped-flow software supplied by Applied Photophysics. All traces could be fitted to the single exponential $F = \alpha(1 - e^{-k_{obs}t})$, where α is the amplitude and k_{obs} is the observed rate.

Halide binding was simulated using the computer program Gepasi, designed by P. Mendes (Gepasi for MS-Windows, version 2.0, release 2.08). This program uses numerical integration to simulate reaction schemes. The Gepasi output was directed to the spreadsheet program Quattro Pro 5.0 for MS-Windows (Borland International, Inc.). Here, the total fluorescence of all enzyme species at each time point was calculated, using a one-third reduction of fluorescence by halide binding. This resulted in simulated fluorescence traces which were fitted in Sigmaplot to calculate observed rates. All programs could be run simultaneously under MS-Windows on a 486 PC.

The programs KINSIM and FITSIM, MS-Windows version, kindly provided by C. Frieden (Frieden, 1994), were used to simulate and fit the fluorescence transient obtained after a single turnover of the enzyme by 1,2-dibromoethane.

RESULTS

Fluorescence Changes During Single Turnover of 1,2-Dibromoethane. Figure 1 shows the fluorescence transient observed upon mixing dehalogenase (15 μM) with 1,2-dibromoethane (13 μM). The initial part of the reaction

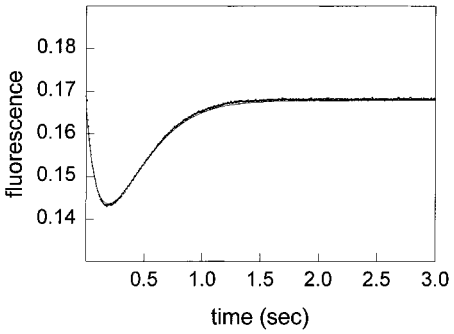

FIGURE 1: Fluorescence transient obtained after rapid mixing of haloalkane dehalogenase (15 μM) and 1,2-dibromoethane (12.5 μM). The solid line represents the fit of the data to Scheme 1 as described in the text.

Scheme 1

$$E + RX \underset{k_{-1}}{\overset{k_1}{\rightleftharpoons}} E.RX \xrightarrow{k_2} E\text{-}R.X \xrightarrow{k_3} E + ROH + X$$

seems to be fast, while the latter part of opposite amplitude is more slow. Rate constants could be derived for a three-step mechanism (Scheme 1) using the program FITSIM and estimates of the relative fluorescence of the different enzyme intermediates. The relative fluorescence of E·RX compared to free enzyme (E) was set at 0.35, based on the degree of quenching by 1,2-dibromoethane observed in an Asp124Gly mutant in which the Michaelis complex accumulates (Pries et al., 1994a). The relative fluorescence of the alkyl−enzyme intermediate (E−R·X) was set at 0.55 based on the quenching observed for the bromide-bound covalent intermediate of a His289Gln mutant enzyme, in which the intermediate is trapped (Pries et al., 1995a).

Fitting the fluorescence transient to Scheme 1 did not result in an unique solution for the k_{-1} and k_2, but the values for k_1 and k_3 converged to stable rates. With a rate constant of 4.5 ± 0.5 s^{-1}, the last step (k_3) was the slowest step in the sequence. Starting the simulation with k_2 as the slow step did converge but led to values of k_1 (0.2 μM^{-1} s^{-1}) below the k_{cat}/K_m (0.3 μM^{-1} s^{-1}), which is the lower limit of k_1 (Fersht, 1985). The last step could be rate-limiting since a k_3 of 4.5 s^{-1} is close to the k_{cat} for 1,2-dibromoethane conversion (3 s^{-1}). It was not possible to fit the transient to a two-step mechanism with E·RX or E−R·X as the central intermediate. In Scheme 1, k_3 represents the rate of hydrolysis of the alkyl−enzyme intermediate and release of alcohol and halide to free enzyme and products. In order to obtain information on the rate of halide release and binding, this was measured directly.

Stopped-Flow Studies of Bromide Binding and Dissociation. Stopped-flow fluorescence experiments were used to study kinetics of the binding of bromide (1−1000 mM) to the dehalogenase (5 μM). The typical fluorescence transients obtained after rapid mixing of enzyme with various concentrations of bromide (1−50 mM) are shown in Figure 2A. The dissociation constant calculated from the steady-state fluorescence reached at the end of each transient resulted in a K_d (10 ± 1 mM) identical to the one obtained by steady-state fluorescence quenching measurement of bromide binding ($K_d = 9.5 \pm 0.5$ mM, not shown), indicating that the conditions of the stopped-flow and steady-state experiments were similar. All fluorescence transients could be fitted to a single exponential. Analysis of the observed rates (k_{obs})

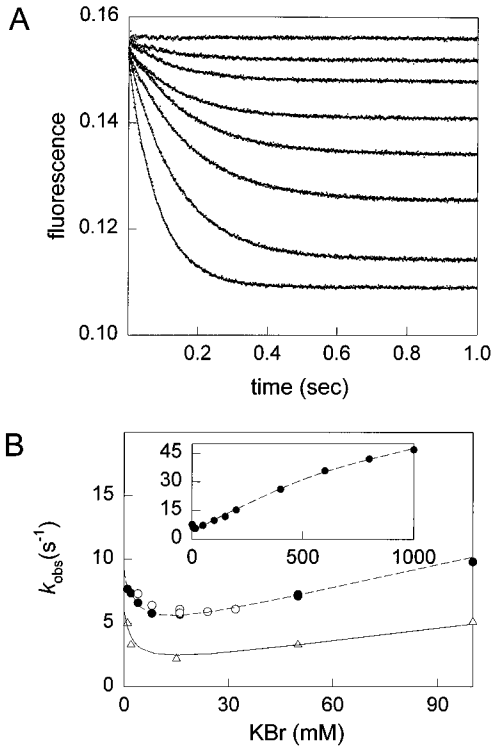

FIGURE 2: Kinetics of bromide binding (1−1000 mM) to haloalkane dehalogenase (5 μM). (A) Fluorescence transients obtained upon binding of bromide. Haloalkane dehalogenase (5 μM) in TEMA buffer was mixed with KBr dissolved in TEMA buffer to give the final concentrations of 0, 1, 2, 4, 8, 16, 50, and 150 mM KBr (going from the top to the bottom). The solid lines represent the best fit to a single exponential. (B) The concentration dependence of the k_{obs} for bromide binding (1−100 mM, ●). The inset displays the complete bromide concentration range used in the experiment (1−1000 mM, ●). The dashed line is the fit obtained by simulation of Scheme 4 (data in Table 1). ○, k_{obs} for enzyme premixed with halide and diluted 1/1 with TEMA to 32, 24, 16, 8, and 4 mM KBr. △, k_{obs} for bromide binding (1, 2, 15, 50, and 100 mM) in ^2H_2O (94.5%, v/v). The solid line is the best fit to Scheme 5 using the data in Table 1.

over the complete concentration range (1−1000 mM KBr) showed a complicated dependence on the halide concentration (Figure 2B). The k_{obs} decreased from 8 s^{-1} at 1 mM KBr to 5 s^{-1} between 15 and 25 mM KBr. There was an increase in the k_{obs} with increasing bromide concentration above 25 mM KBr. At high bromide concentrations (above 600 mM) the k_{obs} leveled off again. Using NaBr instead of KBr and a change of buffer or stopped-flow machine (SLM-Aminco, equipped with stopped-flow unit) did not change the results. Bromide-binding experiments in which the ionic strength was held constant by addition of appropriate amounts of NaF also did not change the outcome of the experiment. NaF did not bind to the active site of the enzyme and did not quench the fluorescence (J. P. Schanstra, unpublished results).

The concentration dependence of the k_{obs} can be interpreted as follows. The decrease in k_{obs} upon increasing bromide concentrations (1−20 mM) is in agreement with a reaction scheme with a slow unimolecular isomerization step followed by a rapid bimolecular step, where the fluorescence of E_{II}·X is quenched (Scheme 2). With this scheme, the k_{obs} decreases at increasing bromide concentration from $k_1 + k_{-1}$ to k_1 (Fersht, 1985). The parabolic increase of k_{obs} with increasing bromide concentration (20−1000 mM KBr) can be accounted for by a reaction scheme with a fast bimolecular step

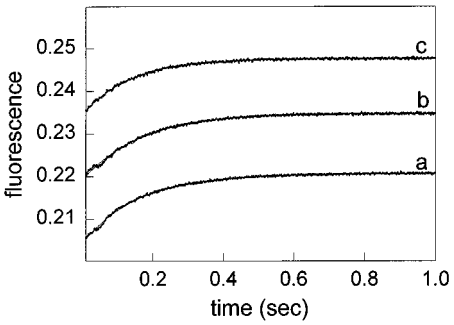

FIGURE 3: Kinetics of bromide dissociation. Haloalkane dehalogenase (5 μM) was premixed with bromide and diluted 1/1 with TEMA buffer. Dilution from 32 to 16 mM (a), 16 to 8 mM (b), and 8 to 4 mM (c) KBr. The solid lines are the best fit to a single exponential.

Scheme 2

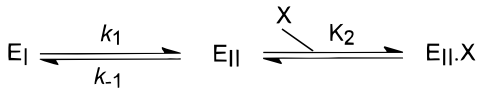

Scheme 3

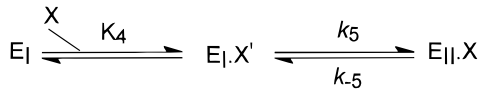

followed by a slow unimolecular step (Scheme 3), where the fluorescence of the E_{II}·X complex is quenched. In this scheme, the k_{obs} changes from k_{-5} to a maximum of $k_5 + k_{-5}$ as the bromide level is increased (Gutfreund, 1972; Johnson, 1986).

To explain the observed dip in the plot of k_{obs} *versus* [Br^-], the k_{obs} should mainly be determined by the route of Scheme 2 at low halide concentrations while at higher concentrations the kinetics of binding are mainly determined by Scheme 3. This is due to a high K_4. Since all traces followed single exponentials, these two routes must operate parallel (Johnson, 1992).

The combined routes can completely explain the observed dependence of the k_{obs} on the bromide concentration. However, fitting this parallel scheme to the observed rates gave rate constants k_1 and k_{-1} and an equilibrium constant K_2 that predict that a significant amount of enzyme should be present as E_{II} both in the absence and at subsaturating concentrations of bromide. This should give a burst in fluorescence change upon bromide addition. Furthermore, if the last step is a rapid equilibrium, there should be a burst in fluorescence change upon dilution of enzyme premixed with bromide. Such bursts were not observed, however (Figures 2A and 3), which may be caused by the fluorescence of E_{II} being quenched or by an additional step in Scheme 2, abolishing rapid equilibrium between halide bound and halide free enzyme. No changes in fluorescence were observed when the pH was changed, although the equilibrium between E_I and E_{II} varied at different pH values. Therefore, there must be a second isomerization step after halide binding which abolishes the rapid equilibrium and reduces the concentration of E_{II} and E_{II}·X (Scheme 4).

This complete scheme is too complex to solve analytically, but several rounds of simulation and fitting of the corresponding exponentials (see Materials and Methods) resulted in rates and equilibrium constants for bromide binding (Table 1; Figure 2B).

Scheme 4

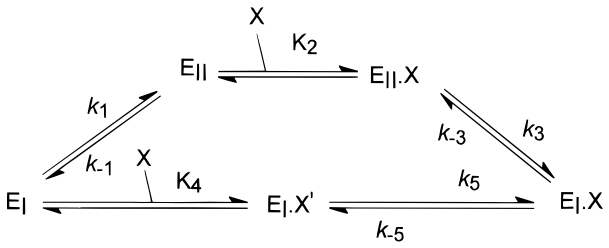

Additional constraints during this repetitive simulation and fitting process were the requirement that only very low amounts of E_{II} and E_{II}·X (1% or less) should be present, that single exponentials were obtained, and that the steady-state fluorescence quenching calculated from the kinetic data should equal the experimental steady-state quenching. The steady-state fluorescence is dependent on the halide concentration according to a normal ligand binding curve:

$$F = F_0 - f_a F_0 \times \frac{k_{-1}k_5(k_3 + k_{-3})}{k_{-1}(k_3k_5 + k_{-3}k_5 + k_3k_{-5})\cdot X + K_4k_3k_{-5}(k_1 + k_{-1})}\cdot X$$

in which the apparent dissociation constant is given by

$$K_d = \frac{K_4k_3k_{-5}(k_1 + k_{-1})}{k_{-1}(k_3k_5 + k_{-3}k_5 + k_3k_{-5})}$$

Since $k_3 \gg k_{-3}$ and $k_{-1} \gg k_1$, this can be simplified to

$$K_d = K_4\frac{k_{-5}}{(k_{-5} + k_5)}$$

The kinetics of the upper route in Scheme 4 is largely determined by the slow k_1 and the slow k_{-3}. The rates of the other steps are fast. This gives single exponentials for the upper route with the data given in Table 1. The value of the equilibrium constant K_2 is dependent on the equilibria [E_{II}]↔[E_I] and [E_{II}·X]↔[E_I·X] and could not be determined because only lower limits were obtained for k_{-1} and k_3. Simulations of Scheme 4 with only E_I·X quenched or with both E_I·X and E_{II}·X quenched resulted only in slight variations in rate and equilibrium constants because of the high k_3 and k_{-1}.

The upper route of Scheme 4 is predominant for bromide binding at low bromide concentrations, whereas the lower route is only kinetically important at high bromide concentrations due to the high K_4. According to Scheme 4 and the data in Table 1, bromide release follows mainly the upper route which is limited by k_{-3}. The rate of k_{-3} (9 ± 1 s^{-1}) is in the same order of magnitude as the steady-state k_{cat} (3 s^{-1}) for 1,2-dibromoethane conversion.

The k_{obs} obtained after fitting single exponentials to fluorescence transients obtained in a series of dilution experiments showed the same dependence on the final bromide concentration as in the corresponding binding experiments (Figure 2B). Scheme 4, and also the other schemes, demand that the observed rate with which the enzyme reaches a new equilibrium after dilution is the same as the rate for halide binding with this same halide concentration. This symmetry in the relaxation times occurs in many cases (Fersht, 1985).

Table 1: Kinetics of Halide Binding[a]

	scheme	K_d (mM)	K_d, calcd (mM)[b]	k_1 (s^{-1})	k_{-1} (s^{-1})	k_3 (s^{-1})	k_{-3} (s^{-1})	K_4 (mM)	k_5 (s^{-1})	k_{-5} (s^{-1})	k_6 (mM^{-1} s^{-1})	k_{-6} (s^{-1})
KBr												
pH 8.5	5	17 ± 1	17	2.2 ± 0.5	>220	>700	7 ± 1.5	–[c]	–	–	0.046 ± 0.002	0.8 ± 0.1
pH 8.2	4	10 ± 1	8	3 ± 0.5	>300	>900	9 ± 1	1466 ± 614	110 ± 20	0.6 ± 0.1	0.06 ± 0.01[d]	0.7 ± 0.1[d]
pH 7.7	4	5.9 ± 0.3	5.9	5 ± 1	>500	>1100	11 ± 2	638 ± 300	85 ± 10	0.8 ± 0.2	–	–
pH 7.2	3	2 ± 0.1	(23)	–	–	–	–	131 ± 25	(55 ± 7)	(12 ± 0.4)	–	–
pH 6.7	3	1 ± 0.1	(2.5)	–	–	–	–	12 ± 1.7	(46 ± 3)	(12 ± 0.8)	–	–
pH 6.3	3	0.67 ± 0.04	0.61	–	–	–	–	3.8 ± 0.5	58 ± 3	11 ± 0.7	–	–
KBr−^2H_2O[e]	5	17 ± 2	17	0.75 ± 0.3	>75	>550	5.5 ± 1	–	–	–	0.035 ± 0.003	0.6 ± 0.05
NaCl[e]	5	75 ± 5	78	3 ± 0.3	>300	>1450	14.5 ± 0.5	–	–	–	0.0085 ± 0.005	0.66 ± 0.03
NaCl−^2H_2O[e]	5	133 ± 7	137	1 ± 0.5	>100	>430	4.3 ± 0.3	–	–	–	0.0044 ± 0.001	0.6 ± 0.1

[a] Rate and equilibrium constants at different pH values in ^1H_2O and in ^2H_2O obtained after fitting of Schemes 4 and 5. See the text for details. Fits are shown in Figures 2B, 4A, and 5A. [b] Calculated K_d values, using the kinetic constants obtained from numerical simulation (see text for details). [c] –, not applicable for scheme used in fit. [d] Scheme 5 used for fit up to 100 mM KBr. [e] Determined at pH 8.2.

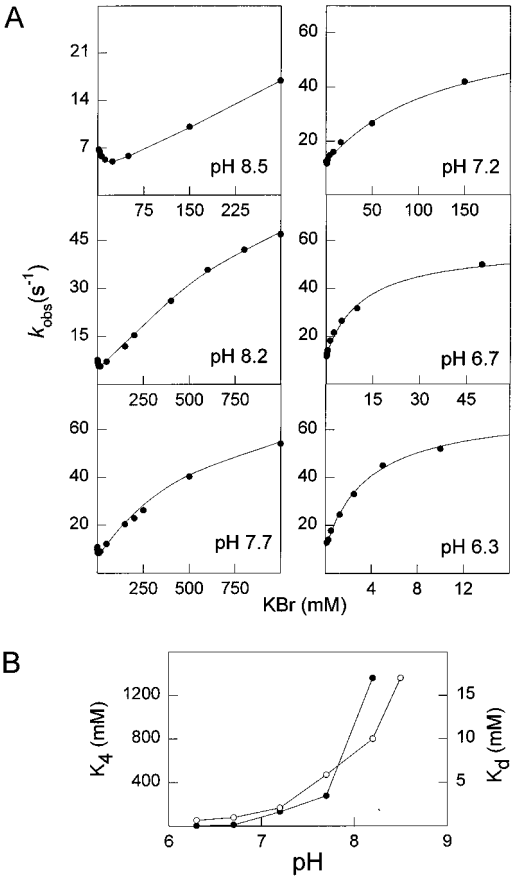

FIGURE 4: Bromide binding to haloalkane dehalogenase (5 μM) at different pH values. (A) Concentration dependence of the k_{obs} for bromide binding at pH 8.5, 8.2, 7.7, 7.2, 6.7, and 6.3. The solid lines are the best fits to Scheme 5 (pH 8.5), Scheme 4 (pH 8.2 and 7.7), and the lower route of Scheme 4 (pH 7.2, 6.7, and 6.3). (B) Dependence of the steady-state experimental K_d (○) and affinity constant K_4 (●) of the lower route in Scheme 4 on the pH.

The affinity of haloalkane dehalogenase for halides increases with decreasing pH (Verschueren et al., 1993c). The complex dependence of the k_{obs} on the bromide concentration was also found at pH 8.5 and pH 7.7 (Figure 4A, Table 1). At lower pH, the importance of the lower route in Scheme 4 increased, since the K_4 decreased from 1360 mM KBr at pH 8.2 to 638 mM at pH 7.7. Below pH 7.2, the data could be fitted by assuming a simple two-step mechanism involving the formation of an initial collision complex, like in Scheme 3. The apparent K_d as obtained by steady-state fluorescence measurements for this scheme is given by

$$K_d = K_4 \frac{k_{-5}}{(k_{-5} + k_5)}$$

The rate constants obtained at pH 7.2 and 6.7 gave a calculated steady-state K_d value that was significantly higher than the one experimentally obtained (Table 1). This is caused by the presence of the upper route, which is kinetically masked at pH 7.2 and pH 6.7 by the lower route. At pH 6.3 the upper route became insignificant since the calculated K_d is in agreement with the experimentally obtained K_d. The importance of the lower route in Scheme 4 is mainly determined by the affinity constant of this route, K_4, which was found to be correlated with the decrease of the overall K_d for bromide binding at lower pH (Figure 4B).

Stopped-Flow Studies of Chloride Binding and Dissociation. Stopped-flow fluorescence analysis of chloride binding showed a similar dependence of the k_{obs} on the chloride concentration (Figure 5A) as was found for bromide binding. The k_{obs} decreased from 12 to 6 s^{-1} from 10 to 150 mM NaCl, followed by a linear increase at higher chloride concentrations. All traces followed single exponentials. No burst in fluorescence was observed upon addition of chloride to free enzyme or dilution of enzyme premixed with chloride (Figure 5B). The decrease of the k_{obs} with increasing chloride concentration (10−150 mM NaCl) can also be explained by the upper pathway in Scheme 4 and thus is comparable to the kinetics of binding at low bromide concentration. The dip in the k_{obs} *versus* concentration plot occurred at higher concentration with chloride than with bromide, however. The rate of binding at high chloride concentrations (from 150 to 1000 mM) followed a linear concentration dependence, in agreement with a simple bimolecular association step. Mechanistically, this could be a two-step process with a hyperbolic dependence of the k_{obs} on the chloride concentration which is not observed experimentally since all chloride concentrations tested fall in the linear part of the curve. This is also suggested by the fact that k_6 (Table 1) is far below the diffusion controlled theoretical value of 10^9 M^{-1} s^{-1} (Fersht, 1985) and indicates a two step mechanism with the formation of an initial collision complex as found with bromide. At low concentrations (20−150 mM), the dependence of the k_{obs} of bromide binding can also be described with a simple bimolecular association step where the value for k_6 corresponds with k_5/K_4 (Table 1, Johnson, 1986).

The complete rate dependence of the k_{obs} on the chloride concentration can be described with Scheme 5 (Table 1). The data were again fitted by numerical simulation yielding

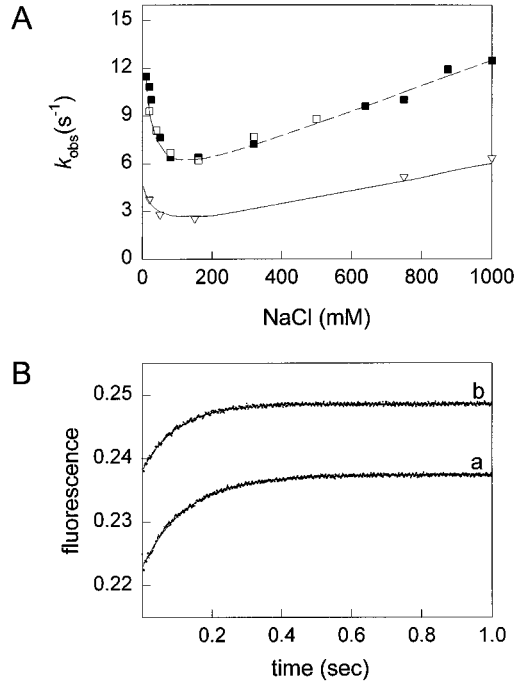

FIGURE 5: Kinetics of chloride binding and release. (A) Concentration dependence of the k_{obs} for chloride binding and release. ■, k_{obs} for binding of chloride (10−1000 mM) to haloalkane dehalogenase (5 μM). The dashed line is the fit obtained by simulation of Scheme 5 (data in Table 1). □, k_{obs} for enzyme premixed with chloride and diluted 1/1 in TEMA to 500, 320, 160, 80, 40, and 20 mM KBr. ▽, k_{obs} for chloride binding (20, 50, 150, 750, and 1000 mM NaCl) in ^2H_2O (94.5%, v/v). The solid line is the best fit to Scheme 5. (B) Kinetics of chloride dissociation. Haloalkane dehalogenase (5 μM) was premixed with chloride and diluted 1/1 in TEMA buffer. From bottom to the top of the figure dilution from 100 to 50 mM (a) and 40 to 20 mM (b) NaCl. The solid lines are the best fit to a single exponential.

Scheme 5

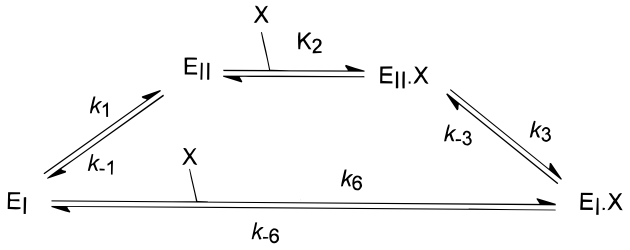

the rates and equilibrium constants given in Table 1 and the best fit shown in Figure 5A. The constraints were that only single exponentials should be obtained, that only low amounts of E_{II} and E_{II}·X should be present (less than 1%), and that at high chloride concentrations (above 600 mM) the slope of the k_{obs} *versus* chloride concentration curve is mainly determined by k_6 (Scheme 5). A further constraint was the experimental K_d obtained by steady-state fluorescence quenching, which is given by

$$K_d = k_3 k_{-6} \frac{(k_1 + k_{-1})}{k_{-1} k_6 (k_3 + k_{-3})}$$

and simplifies to

$$K_d = \frac{k_{-6}}{k_6}$$

when $k_3 \gg k_{-3}$ and $k_{-1} \gg k_1$.

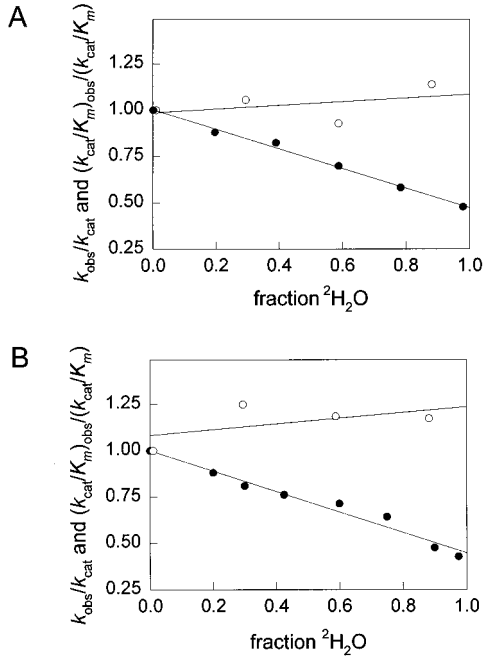

FIGURE 6: Solvent (^2H_2O) kinetic isotope effects on haloalkane dehalogenase activity. The observed k_{cat} (k_{obs}) and k_{cat}/K_m [$(k_{cat}/K_m)_{obs}$] as the fraction of the k_{cat} and k_{cat}/K_m observed in ^1H_2O was determined at different $^2H_2O/^1H_2O$ ratios. (A) ●, k_{obs}/k_{cat}, and ○, $(k_{cat}/K_m)_{obs}/(k_{cat}/K_m)$ for 1,2-dibromoethane conversion. (B) ●, k_{obs}/k_{cat}, and ○, $(k_{cat}/K_m)_{obs}/(k_{cat}/K_m)$ for 1,2-dichloroethane conversion.

The fastest pathway for chloride release via Scheme 5 is again the upper route, which is limited by k_{-3} (14.5 ± 0.5 s^{-1}). This is not as close to the steady-state k_{cat} (3.5 s^{-1}) for conversion of the corresponding substrate (1,2-dichloroethane) as was found for bromide release.

Effects of ^2H_2O on Substrate Conversion and Halide Binding. When the dehalogenase reaction was performed in increasing concentrations of ^2H_2O, the k_{cat} decreased both for 1,2-dibromoethane and 1,2-dichloroethane (Figure 6A,B). A ^2H_2O solvent kinetic isotope effect on k_{cat} often indicates the cleavage of H−X (X = C, N, O) bonds in the rate-determining step. Cleavage of a H−X bond in the dehalogenase reaction occurs during hydrolytic cleavage of the alkyl−enzyme intermediate which is facilitated by proton-abstraction from water by histidine 289 (Verschueren et al., 1993b; Pries et al., 1995a). Since the kinetics of halide binding suggested that halide release was limiting the k_{cat}, the ^2H_2O isotope effect could also be caused by an effect on the kinetic constants of Schemes 4 and 5.

There was no effect of ^2H_2O on the k_{cat}/K_m (Figure 6A,B) indicating that only the last steps of the catalytic cycle were influenced by ^2H_2O as the solvent. For a three-step mechanism and steady-state initial velocity conditions (Scheme 1), $K_m = K_s k_3/(k_2 + k_3)$, $k_{cat} = k_2 k_3/(k_2 + k_3)$, and $k_{cat}/K_m = k_2/K_s$. Thus, there is no effect of ^2H_2O on k_{cat}/K_m when only k_3 is affected. Extension of reaction Scheme 1 by adding a reversible halide release step also predicts no solvent ^2H_2O effect on k_{cat}/K_m if only the last step would be influenced.

We studied the kinetics of halide binding in ^2H_2O to determine whether there is an effect on the rate of binding of bromide (Figure 2B) and chloride (Figure 5A). A clear effect of ^2H_2O on the k_{obs} was found for both bromide and chloride. All fluorescence transients could be fitted by single exponentials. Extraction of the rate and equilibrium constants in ^2H_2O showed that both slow isomerization steps,

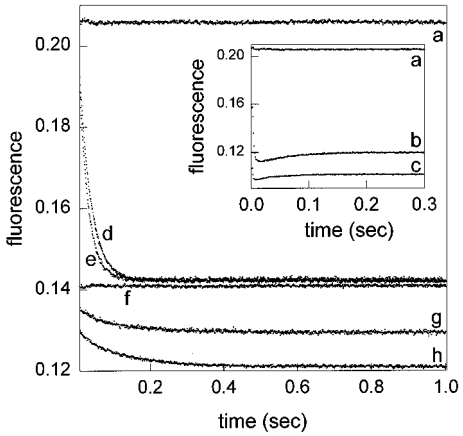

FIGURE 7: Binding of 1,2-dibromoethane to free and halide-bound enzyme. Free enzyme (5 μM) in TEMA was mixed with TEMA (a), with 500 and 750 mM of KBr (d, e), and with 1 mM and 5 mM 1,2-dibromoethane (inset: b and c, respectively) in TEMA. Enzyme (5 mM) in TEMA premixed with halide (500 mM KBr) was mixed with 500 mM KBr (f), 500 mM KBr + 1 mM 1,2-dibromoethane in TEMA (g, $k_{obs} = 8.1 \pm 0.4$ s^{-1}) and 500 mM KBr + 5 mM 1,2-dibromoethane in TEMA (h, $k_{obs} = 8.8 \pm 0.5$ s^{-1}).

(k_1) and (k_{-3}), were affected by use of ^2H_2O (Table 1). The isomerization step determining the halide off-rate (k_{-3}) was reduced by 50% and 70% for bromide and chloride, respectively, corresponding to a reduction in k_{cat} by 50% in ^2H_2O for both 1,2-dibromoethane and 1,2-dichloroethane.

To check whether the increased viscosity caused by the high ^2H_2O concentration could account for the effect on the rate of halide binding, the experiments were also performed in the presence of 6% glycerol, the viscosity-equivalent of 95% ^2H_2O. There was no significant effect on the kinetics of halide binding, indicating that the effect of ^2H_2O is not due to higher viscosity.

Binding of Substrate to Halide-Bound Enzyme. If release of halide limits the catalytic rate for 1,2-dibromoethane and 1,2-dichloroethane, then binding of substrate to enzyme saturated with halide should be slow. We tested binding of 1,2-dibromoethane to free enzyme and enzyme premixed with bromide (Figure 7).

Binding of 1,2-dibromoethane (1 and 5 mM) to halide free enzyme occurred almost instantaneously. The largest part of the transient occurred within the dead time of the instrument (±1 ms) followed by a small fluorescence increase after which the reaction quickly reached a steady-state fluorescence level (Figure 7, inset). Gradually increasing the concentration of 1,2-dibromoethane (from 1 to 10 mM) caused an increase in amplitude and rate of the first part of the fluorescence transient (not shown). The concentration dependence of this first fast phase suggests that this is correlated to the rapid binding of the substrate. With active site mutants of the dehalogenase it was found that the fluorescence of the Michaelis complex and alkyl−enzyme intermediate (Pries et al., 1994a, 1995a) was lower than that of the halide bound enzyme (Verschueren et al., 1993c). Furthermore, 1,2-dibromoethane displays also some non-specific quenching as observed before with a dehalogenase mutant in which the alkyl−enzyme intermediate accumulates (D. B. Janssen and J. Kingma, unpublished results). The difference in quenching between bromide and 1,2-dibromoethane was similar in the wild type enzyme and allowed the design of an experiment in which the rate of displacement of halide by substrate can be measured.

To ensure that all enzyme was in the halide-bound form, the dehalogenase was premixed with 500 mM bromide, which is 50-fold above the steady-state K_d. Increasing the bromide concentration to 750 mM only increased the rate of binding and not the amplitude (Figure 7), indicating that the enzyme was indeed saturated. Binding of 1,2-dibromoethane to enzyme saturated with bromide (500 mM) was slow (Figure 7) with a $k_{obs} = 8.1 \pm 0.4$ s^{-1} for 1 mM 1,2-dibromoethane and a $k_{obs} = 8.8 \pm 0.5$ s^{-1} for 5 mM 1,2-dibromoethane. The slow fluorescence transient caused by binding of 1,2-dibromoethane to halide bound enzyme did not start at the fluorescence level of enzyme premixed with 500 mM KBr (Figure 7). The loss of half of the amplitude within the dead time of the instrument can be explained by the nonspecific quenching of 1,2-dibromoethane.

The observed rate of binding of 1,2-dibromoethane to halide-bound enzyme (8 s^{-1}) was close to the rate of bromide release (9 s^{-1}) and in the same order of magnitude as the k_{cat} (3 s^{-1}). Unfortunately, a similar displacement experiment is difficult to perform with 1,2-dichloroethane and chloride since the high K_d for chloride makes it impossible to completely saturate the enzyme with chloride.

DISCUSSION

Rate-Limiting Step of Haloalkane Dehalogenase Is at the End of the Reaction Sequence. The results presented in this manuscript indicate that the slowest step in the kinetics of 1,2-dibromoethane and 1,2-dichloroethane conversion by haloalkane dehalogenase at saturating substrate concentration is located at the end of the reaction sequence, i.e., hydrolysis of the alkyl−enzyme intermediate or product release. This conclusion is supported by a single-turnover experiment, solvent kinetic isotope effects, and X-ray crystallographic studies.

The fluorescence transient obtained from a single-turnover experiment with 1,2-dibromoethane could only be described with a slow last step. Although this technique allows no discrimination between the rates of alkyl−enzyme hydrolysis or product export it indicated that the slow step occurred after substrate binding and cleavage of the carbon−halogen bond. This experiment could only be performed with 1,2-dibromoethane, not with 1,2-dichloroethane, since the latter has a too high K_m (0.6 mM), but we have several reasons to believe that both substrates have a similar rate-limiting step at the end of the reaction sequence. First, while the turnover numbers were very close to each other (3 and 3.5 s^{-1} for 1,2-dibromoethane and 1,2-dichloroethane, respectively), the K_m values for both substrates differ strongly (10 μM for 1,2-dibromoethane and 0.6 mM for 1,2-dichloroethane). Second, a clear solvent kinetic isotope effect on k_{cat} but not on k_{cat}/K_m was found both with 1,2-dibromoethane and 1,2-dichloroethane. On the basis of the steady-state kinetic parameters, this suggests that k_3 in a three-step mechanism (Scheme 1), and k_3 and/or k_4 in a four-step mechanism are involved in the rate-determining step.

Thus, the possible slow steps in the reaction sequence of the dehalogenase are hydrolysis of the alkyl−enzyme intermediate and/or halide release. The latter was studied with stopped-flow fluorescence.

Halide Release Is Limited by an Enzyme Isomerization. Binding of halide to haloalkane dehalogenase displayed a

complex dependence of the observed rate on the halide concentration. This could be explained by the presence of two parallel routes, one route in which a slow enzyme isomerization preceded a rapid halide binding step, and a second route in which the rapid formation into an initial collision complex is followed by a slow enzyme isomerization. The first route dominated at low halide concentrations while the latter prevailed at higher concentrations. The halide binding and release rates extracted from this complex dependence showed that the rate of halide release could limit the k_{cat}. The rate of bromide release was close to the steady-state k_{cat}, and the solvent kinetic isotope effect of ^2H_2O on k_{cat} was also found back in the rate of halide release. Both the k_{cat} for 1,2-dibromoethane and the rate of bromide release were about 50% lower in ^2H_2O than in ^1H_2O. Furthermore, at 5 mM 1,2-dibromoethane the observed rate of substrate binding reduced from faster than 700 s^{-1} (within the dead time of the stopped-flow instrument) to free enzyme, to 8 s^{-1} to halide-bound enzyme in a displacement experiment. The k_{cat} for 1,2-dichloroethane conversion was less close to the chloride off-rate, although the presence of a solvent kinetic isotope effect both on k_{cat} and on the rate of chloride release suggested that these rates are correlated. This indicates the presence of another slow step in the reaction sequence for 1,2-dichloroethane conversion since two subsequent slow steps result in a significant reduction of the overall rate. The other halide release route (the lower route in Schemes 4 and 5) was found to be even slower than the upper route. Only a small amount of halide (<8% bromide and <5% chloride) will exit *via* this route at low halide levels in the buffer. The fact that halide release itself is not rate-limiting allows a 10-fold difference in affinity for bromide and chloride with similar halide off-rates.

A slow enzyme isomerization followed by rapid ligand binding was also found for binding of $MgCl_2$ to *Eco*RV complexed to DNA (Baldwin et al., 1995), binding of K^+ to ATPase (Pratap et al., 1991), and binding of proflavin to α-chymotrypsin (Fersht & Requena, 1971). Only in the last case were rates derived. The slow step in binding of proflavin to α-chymotrypsin is the interconversion between two different conformations of the enzyme that occur both at significant concentrations and not the actual binding of the ligand.

Nature of the Enzyme Isomerization. The active site of the dehalogenase is buried in the protein with no obvious route for substrate entrance or product release. However, binding of the uncharged substrate and probably also release of the uncharged alcohol, which both have larger van der Waals volumes than halide, are fast. Only release of the charged halide ion out of the buried active site was found to be slow since it required an enzyme isomerization. The route for substrate entrance and alcohol release is apparently not suitable for halide release. Probably, the uncharged alkyl halide and alcohol can diffuse through openings formed by fluctuations or small motions, whereas the halide ion can only leave the buried active site after solvation by water. Halides are not nonspecific collisional quenchers such as the polar non-ionic acrylamide, which quenches all tryptophans in the dehalogenase (Verschueren et al., 1993c); halide ions only quench the fluorescence of accessible tryptophans because they cannot diffuse freely through the enzyme. Transport of halide from and to the surrounding water may need a specific route, or water may be required to enter the active site to solvate the halide ion. A specific halide export route could involve binding to charged residues such as arginine, which would assist the halide ion to reach the solvent, as was found in various transmembrane anion transporters (Hannon & Anslyn, 1993; Rüdiger et al., 1995). There is no arginine close to the halide binding site. The only positively charged residue close enough to interact with the halide is Lys176 (Verschueren et al., 1993b,c). Lysine is, however, a less good anion binder than arginine as was shown in halorhodopsin (Rüdiger et al., 1995).

A way to solvate the halide would be allowing water to enter the active site. A possible route for this is the entrance of water *via* a tunnel extending from the solvent close to the active site cavity as proposed by X-ray crystallography (Verschueren et al, 1993a). Another route could possibly be formed by a conformational change of part of the cap domain, which possesses considerable flexibility since it allows binding and conversion of large substrates such as 1-bromooctane (Pries et al., 1994b). Large substrate-induced structural changes were observed in mobile surface loops of several lipases (Jaeger et al., 1994), which, like the dehalogenase, belong to the α/β-hydrolase fold enzymes. The suggestion that a conformational change of the cap domain or parts of it are involved in halide release and binding is supported by the observation that ^2H_2O as the solvent slowed down the enzyme isomerization step preceding halide release and binding. ^2H_2O is known to increase the strength of hydrogen bonds and to enhance hydrophobic interactions, and it is well known that ^2H_2O protects several proteins against thermal denaturation (Tuena de Gómez-Puyou et al., 1978; Masson & Laurentie, 1988; Antonino et al., 1991). This overall stabilizing effect of ^2H_2O supports a conformational change as the rate-limiting step.

ACKNOWLEDGMENT

We thank the members of the Protein Crystallography and Molecular Dynamics groups from the University of Groningen for many stimulating discussions. We thank Dr. A. Driessen for using the stopped-flow equipment in his laboratory to perform the initial binding experiments and A. Wieringa for obtaining the k_{cat}/K_m values for Figure 6.

REFERENCES

Antonino, L. C., Kautz, R. A., Nakano, T., Fox, R. O., & Fink, A. L. (1991) *Proc. Natl. Acad. Sci. U.S.A. 88*, 7715−7718.

Baldwin, G. S., Vipond, B. I., & Halford, S. E. (1995) *Biochemistry 34*, 705−714.

Fersht, A. R. (1985) *Enzyme Structure and Mechanism*, 2nd ed., W. H. Freeman, New York.

Fersht, A. R., & Requena, Y. (1971) *J. Mol. Biol. 60*, 279−290.

Franken, S. M., Rozeboom, H. J., Kalk, K. H., & Dijkstra, B. W. (1991) *EMBO J. 10*, 1297−1302.

Frieden, C. (1994) *Methods Enzymol. 240*, 311−322.

Gutfreund, H. (1972) *Enzymes: Physical Principles*, John Wiley, London.

Jaeger, K. E., Ransac, S., Dijkstra, B. W., Colson, C., van Heuvel, M., & Missot, O. (1994) *FEMS Microbiol. Rev. 15*, 29−63.

Janssen, D. B., Pries, F., van der Ploeg, J., Kazemier, B., Terpstra, P., & Witholt, B. (1989) *J. Bacteriol. 171*, 6791−6799.

Johnson, K. A. (1986) *Methods Enzymol. 134*, 677−705.

Johnson, K. A. (1992) *The Enzymes 20*, 1−61.

Kennes, C., Pries, F., Krooshof, G. H., Bokma, E., Kingma, J., & Janssen, D. B. (1995) *Eur. J. Biochem. 228*, 403−407.

Keuning, S., Janssen, D. B., & Witholt, B. (1985) *J. Bacteriol. 163*, 635−639.

Masson, P., & Laurentie, M. (1988) *Biochem. Biophys. Acta 957*, 111−121.

Ollis, D. L., Cheah, E., Cygler, M., Dijkstra, B. W., Frolow, F., Franken, S. M., Haral, M., Remington, S. J., Silman, I., Schrag, J., Sussman, J. L., Verschueren, K. H. G., & Goldman, A. (1992) *Protein Eng. 5*, 197−211.

Pratap, P. R., Robinson, J. D., & Steinberg, M. I. (1991) *Biochim. Biophys. Acta 1069*, 288−289.

Pries, F., Kingma, J., Pentenga, M., van Pouderoyen, G., JeronimusStratingh, C. M., Bruins, A. P., & Janssen, D. B. (1994a) *Biochemistry 33*, 1242−1247.

Pries, F., van den Wijngaard, A. J., Bos, R., Pentenga, M., & Janssen, D. B. (1994b) *J. Biol. Chem. 269*, 17490−17494.

Pries, F., Kingma, J., Krooshof, G. H., Jeronimus-Stratingh, C. M., Bruins, A. P., & Janssen, D. B. (1995a) *J. Biol. Chem. 270*, 10405−10411.

Pries, F., Kingma, J., & Janssen, D. B. (1995b) *FEBS Lett. 358*, 171−174.

Rüdiger, M., Haupts, U., Gerwert., K., & Oesterhelt, D. (1995) *EMBO J. 14*, 1599−1606.

Schanstra, J. P., Rink, R., Pries, F., & Janssen, D. B. (1993) *Protein Expression Purif. 4*, 479−489.

Studier, F. W., Rosenberg, A. H., Dunn, J. J., & Dubendorff, J. W. (1990) *Methods Enzymol. 185*, 60−89.

Tuena de Gómez-Puyou, M., Gómez-Puyou, A., & Cerbon, J. (1978) *Arch. Biochem. Biophys. 187*, 72−77.

Verschueren, K. H. G., Franken, S. M., Rozeboom, H. J., Kalk, K. H., & Dijkstra, B. W. (1993a) *J. Mol. Biol. 232*, 856−872.

Verschueren, K. H. G., Seljée, F., Rozeboom, H. J., Kalk, K. H., & Dijkstra, B. W. (1993b) *Nature 363*, 693−698.

Verschueren, K. H. G., Kingma, J., Rozeboom, H. J., Kalk, K. H., Janssen, D. B., & Dijkstra, B. W. (1993c) *Biochemistry 32*, 9031−9037.

BI952904G